



ELSEVIER

Available online at www.sciencedirect.com

 ScienceDirect

Proceedings of the Combustion Institute 33 (2011) 2489–2496

Proceedings
of the
Combustion
Institute

www.elsevier.com/locate/proci

Analysis and measurement of candle flame shapes

P.B. Sunderland^a, J.G. Quintiere^{a,*}, G.A. Tabaka^b, D. Lian^c,
C.-W. Chiu^d

^a Department of Fire Protection Engineering, The University of Maryland, College Park, MD 20742-3031, USA

^b Hughes Associates, Baltimore, MD 21227-1652, USA

^c Chinese People's Armed Police Force Academy, Langfang, Hebei, China

^d Taiwan Police College, Taipei City 11696, Taiwan, ROC

Available online 6 October 2010

Abstract

A combined analytical and experimental study was performed to determine the length and width of a candle flame. Measurements were made of laminar steady flames from photographs of straight-wick candles composed of *n*-tetracosane and normal paraffin waxes. The wicks studied ranged in diameter from about 1 to 9 mm, and in height from about 2 to 10 mm, with aspect ratios (diameter to length) of 0.1 to 2. The flame length from the pool surface and the flame width at the top of the wick were found. It was also noted and recorded that the flame attachment point along the vertical wick varied. The attachment point was found to depend on the aspect ratio of the wick. A model based on stagnant layer burning for a finite cylinder was used, along with the Roper laminar burner model for flame height. With slight adjustment to a constant, the width of the flame was well predicted, and the prediction for the flame height was about 60% too high and offset. In addition, the model gave insight to produce an accurate simple correlation for flame height in terms of wick aspect ratio and Rayleigh number.

© 2010 The Combustion Institute. Published by Elsevier Inc. All rights reserved.

Keywords: Candle; Combustion; Flame height; Flame width; Wick

1. Introduction

A candle flame serves to exemplify the basic nature of a diffusion flame in the study of fire. It involves the evaporation of a liquid fuel from a porous surface, and, differing from uncontrolled fire, quickly reaches a steady state. Faraday [1], in his profound lectures of 1850, presents the candle to contain the science of the known universe at

that time. His lectures serve to explain the workings of a candle and related science, and Takahashi [2] gives a more modern explanation. Surprisingly, a systematic study of candle flames has not been presented before. Yet curiosity in the behavior of candle flames prompted a study of their behavior in microgravity [3]. Moreover, simple equations are not available to predict the shape of a candle flame, yet we expect unpublished empirical results must exist in the industry.

Although the candle flame presents a simple example of a diffusion flame, its burning is still complicated by the nature of its finite cylindrical wick. Kosdon et al. [4] performed the closest systematic study of a candle by studying burning on a vertical cylindrical surface; however, their

* Corresponding author. Address: Department of Fire Protection Engineering, The University of Maryland, 3104 J.M. Patterson Building, College Park, MD 20742-3031, USA. Fax: +1 301 405 9383.

E-mail address: jimq@umd.edu (J.G. Quintiere).

Nomenclature

B	Spalding B number
c_p	specific heat of gas at constant pressure
D	diameter of the wick
g	gravitational acceleration
h_c	heat transfer coefficient
h_{fg}	enthalpy of vaporization
k	thermal conductivity
L	length of wick from its base
L_f	length of flame
\dot{m}	mass flow rate
M	molecular weight
n	empirical data fit parameter
Nu	Nusselt number
Ra	Rayleigh number based on D
s	stoichiometric oxygen–fuel mass ratio
S	stoichiometric air–fuel molar ratio

T	temperature
W_f	maximum diameter of the flame

Greek and other symbols

α	thermal diffusivity
β	coefficient of volumetric expansion
λ	see Eq. (13)
ν	kinematic viscosity
Δh_c	enthalpy of combustion

Subscripts

b	relating to burn region
F	fuel
f	flame
ox	oxygen
∞	ambient

cylinders had large aspect ratios (D/L). Consequently, their modeling was made simpler as they could approximate the cylinder as a flat surface. In contrast, candlewicks generally have aspect ratios of about 0.1–1, and therefore consideration of the curvature effect becomes important. Also the smallness of the wick diameter (~ 1 mm) can limit the approximation of boundary layer flow. Moreover, the candle flame around the wick is three-dimensional. Therefore only with recent computational advances have fundamental numerical solutions been employed. Riley [5] used the flame sheet model for steady burning on candlewicks. T'ien and coworkers [6,7] have modeled the capillary action in the wick along with flame kinetics and radiation. Hamins et al. [8] used the popular FDS code to model a candle flame, including the bent geometry of a wick. They also measured the heat flux from a candle flame, and showed that its heat flux could be above 100 kW/m^2 even 10 mm above the visible flame tip. This heat flux feature of the candle flame makes it prone to accidentally start fires, as wood is capable of auto-ignition above 40 kW/m^2 . Therefore, understanding the height and width of a candle flame is important for its industrial design, and also in understanding its ignition potential for fire safety.

Motivated by curiosity and the lack of systematic data, this study was begun to experimentally examine the shape of steady candle flames with wicks in the range of $D/L \sim 0.1$ –2. Once the data were assembled, we sought to explain the results. As the candle flame is generally laminar and gives steady burning of a liquid without significant radiation effects, the B -number approach can be used to explain aspects of its general burning. Spalding [9] illustrates such B -number modeling for spheri-

cal droplets, and Pagni for flat and cylindrical surfaces [10]. Simple analytical equations can follow for predicting the height and width of the candle flames based on the size of the wick and the properties of the wax.

2. Experiments

Laboratory experiments were conducted in which five different wick diameters were molded into candles with various lengths of wick exposed above the plane of solid wax. The wicks are not self-trimming and are designed to remain straight and vertical. Allan et al. [11] describe similar experiments in which the smoke points of candle flames were measured. In the experiments presented here only steady laminar non-smoking candle flames were recorded. When steady state burning was achieved, a high-resolution photograph was taken of the flame. No measurements of mass loss, temperature or velocity were obtained, as the purpose was only to determine the extent of the luminous region of flame under the assumption that the wick geometry would be the governing influence. Two waxes were used, normal paraffin and n -tetracosane. Paraffin wax is a mixture that can contain the pure substance n -tetracosane. Table 1 gives property data where available for n -tetracosane and typical paraffin wax. It can be seen that tetracosane is a good pure property surrogate for paraffin.

Once the catalog of photographs was uploaded to a personal computer, they were analyzed to obtain flame measurements. Figure 1 gives a schematic of terms considered for the flame measurements, and Figs. 2 and 3 give examples of typical flame photographs. The photographic image represented in pixels could then be

Table 1
Wax properties: *n*-tetracosane and paraffin.

Property	<i>n</i> -Tetracosane [12]	Paraffin [8]
Carbon number, <i>n</i> , C_nH_{2n+2}	24	19–36
Melting point (°C)	50	48–68
Boiling point (°C)	391	350–430
Specific heat, liquid (kJ/kg K)	2.3	2.98
Heat of vaporization (kJ/g)	0.62	–
Heat of combustion (kJ/g)	45.3	43.6
Stoichiometric oxygen/fuel mass (g/g)	3.46	~3.29
Molecular weight (g/mol)	339	350–420
<i>B</i> number in air	1.89	–

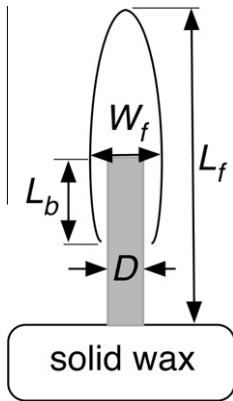


Fig. 1. Schematic of the candle flame.

converted into precise dimensions (mm). The following dimensions were recorded for each photograph:

- (1) Length of the wick above the molten wax pool, L .
- (2) Diameter of the wick at the vertical midpoint, D .
- (3) Flame height above the wax pool, L_f .
- (4) Flame diameter of the top of the wick, W_f .
- (5) Attachment point, or length of the burning region, L_b .

The dry wick diameter was much less than its corresponding liquid saturated wick, and the top of the saturated wick could be up to 0.3 mm bigger than its mid-diameter. For this reason the



Fig. 2. Photograph of typical thin wick flame, $D = 1.13$ mm.



Fig. 3. Photograph of typical thick wick flame, $D = 7.66$ mm.

wick dimensions could not be precisely controlled, but within 1 mm or less the data sets could be grouped into approximately constant diameter sets. The tetracosane wick diameters fell into four clusters: (1) 0.9–1.16 mm, (2) 3.1–3.5 mm, (3) 4.3–4.9 mm, and (4) 7.5–8.5 mm. For the paraffin, this emerged as three clusters: (1) 0.73–1.5 mm, (2) 3.1–4.0 mm, and (3) 5.0–5.2 mm. Each data point is an average of the mid and top of the saturated wick. Analysis was based on these parameter sets.

The photographic measurement technique offers several benefits. First, all dimensions of the flame are available at one particular instant in time. That is, the width and length are presented as a couple, rather than having been measured sequentially, introducing error. Second, measuring the width and height of a flame by a ruler is difficult, and may affect gas flow or introduce cooling effects. Third, an electronic record is made that can be checked in the future. Finally, the high-resolution camera produces images that can be measured very precisely. A conversion factor of 1 mm per 34 pixels was employed, so measurements should have an accuracy of one half-pixel (± 0.059 mm); however, the actual error in measurement can be higher. Sources of

potential error are threefold: First, the base of the candle flame as measured has a faint blue corona that does not appear clearly in digital photographs. This makes discerning the flame attachment point particularly difficult. Second, despite attempts to produce steady flames, flicker and drafts still do occasionally coincide with the photograph. Third, the physical endpoints to measure are sometimes difficult to discern, especially in flame regions that are not sharply defined. Finally, the wick shapes are not ideal as they could not always be aligned perfectly to gravity, nor do candle wicks have the uniform cylindrical shapes with constant diameters and plane ends. We believe measurements are accurate to within about 0.1 mm.

3. Experimental results

Results are shown in Figs. 4a and 4b for the flame length and width against wick height, accordingly. Companion results are shown for (a) tetracosane and (b) paraffin on graphs of the same scale in Figs. 4a and 4b. The data are arranged for the cluster diameter regions that nominally represent nearly constant diameter wicks. Power law fits have been processed for each diameter set to indicate quantitative behavior. Flame length increases more strongly with wick length as the diameter increases, and the tetracosane flames are slightly taller than the corresponding paraffin flames. There are five data for the longest and smallest diameter tetracosane flames that appear to have resulted from the wick possibly drying out and are labeled, accordingly. Dry out is suspected, as flame height appears to level out. These data will be subsequently discarded in any comparison to modeling, as we do not

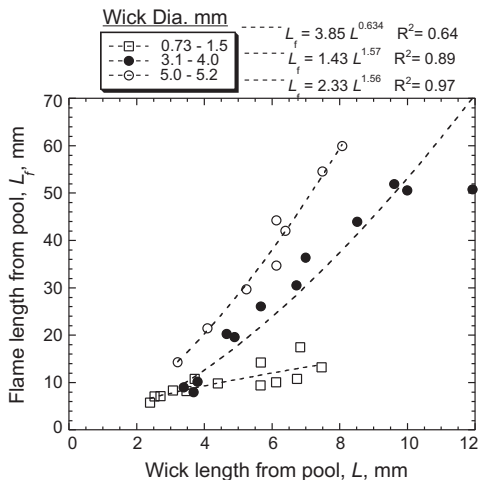


Fig. 4b. Flame height for paraffin with trend lines.

purport to model this effect. It might be observed, however, that dry out seems to occur for aspect ratios (D/L) of less than 0.15, and that flames might not survive for wicks shorter than about 1 mm.

The measured flame width consists of the horizontal distance at the top of the wick across the entire flame. This position appears to be the maximum diameter of the candle flame. It is the location at the end of the boundary layer for the cylindrical flame, and the start of the flame for the “pool” above. This pool fire is fed by the excess fuel from the cylindrical boundary layer and from the evaporated liquid wax from the circular wick top. The tetracosane flames are wider than the corresponding paraffin flames as shown in Figs. 5a and 5b accordingly, and the flame

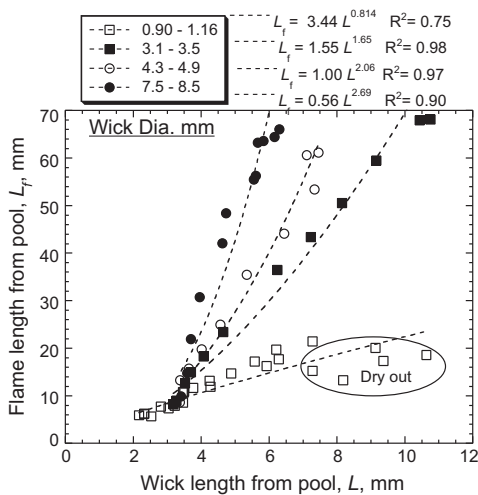


Fig. 4a. Flame height for tetracosane with trend lines.

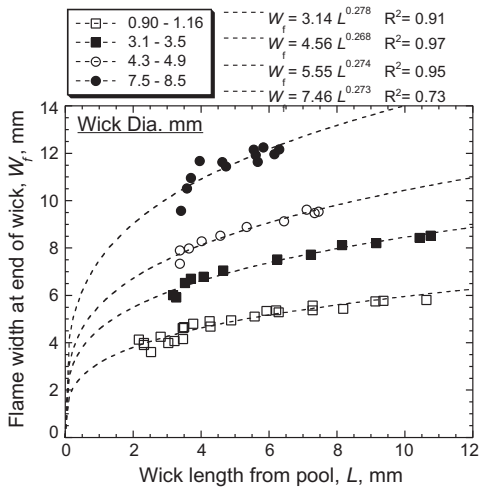


Fig. 5a. Flame width for tetracosane with trend lines.

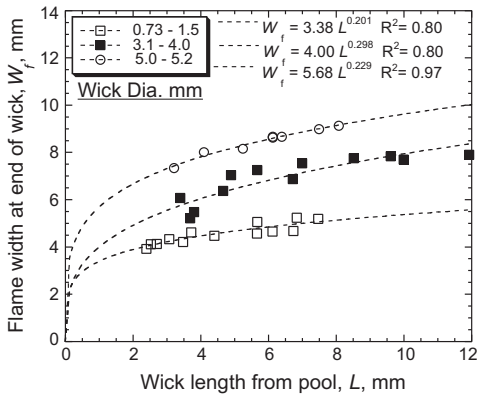


Fig. 5b. Flame width for paraffin with trend line.

widths follow nearly a 1/4-power (0.2–0.3) with wick length for all diameters as expected from laminar boundary behavior. The flame width appears to revert to the wick diameter as L tends to zero.

The flame attachment point on the vertical wick cylinder was an interesting result. It is measured here as the burn length along the cylindrical wick to its top, L_b . The remaining portion of the wick below does not support a flame, and this “quenched” region varied from about 1.5 to 6 mm for these tests. It is not a constant standoff distance from the pool of the liquid wax at the base of the wick. Figure 6 presents the ratio of burning length to the full wick length (L_b/L) for the tetracosane and paraffin plotted against the wick aspect ratio. The relative burning length decreases as the wick diameter increases. For thin wicks, up to 80% of the wick can support a flame, but for thick wicks this could reduce to 20%. This might be explained by considering the larger pool fire at the top as the wick diameter increases. The wider flame has larger buoyancy that can cause an

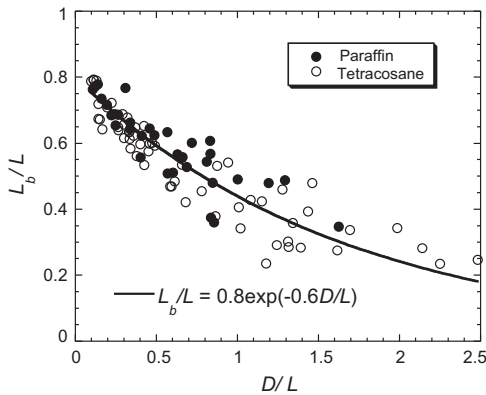


Fig. 6. Normalized burn length against wick aspect ratio with fit.

increase in the flow velocity. The increased speed is likely responsible for causing the flame attachment point to rise along the wick. This is a complex problem to model; however, for purposes here, a fit of the data will suffice as indicated in Fig. 6:

$$\frac{L_b}{L} = 0.8e^{-0.6D/L}. \quad (1)$$

This result is essential for our modeling, as the cylindrical burn length is needed.

4. Model

Initially, a more involved model was attempted than is presented here [12]. Although that model was not completely successful, it laid the foundation for the current analysis, and can be examined to give more details of the solution basis. The approach here is to consider the cylindrical wick combustion and the burning at the top of the wick to be described by a stagnant boundary layer flame sheet model that utilizes heat transfer correlations from the literature to find the boundary layer thickness. The flame height is based on the laminar burner model of Roper et al. [13] that considers the flame height to be linearly related to the fuel flow rate.

The Roper model result for a circular burner diffusion flame, governed by natural convection, gives the height above the port as [13]:

$$L_f(\text{mm}) = 1.33 \times 10^{-3} \left(\frac{s}{\text{mm}^2} \right) \frac{\dot{m}_F}{\rho_F \ln(1 + 1/S)}, \quad (2)$$

where \dot{m}_F is the total fuel mass flow rate and ρ_F is the fuel supply density in appropriate units. S is the stoichiometric molecular air to fuel ratio, given in terms of molecular weights and the mass oxygen to fuel stoichiometric ratio, s , as

$$S = \frac{M_F}{M_{air}} \frac{s}{Y_{ox,\infty}}. \quad (3)$$

Equation (2) is applied to the candle with the fuel supplied as the sum from two locations: (1) the evaporation from the top of the wick and from (2) the cylindrical side. As the fuel supply point is distributed for the candle, the Roper equation cannot be taken as perfectly applicable, but the flame height for the candle will still be linearly proportional to the total fuel flow rate in laminar flow. Equation (2) is made dimensionless, approximated for S large (~ 180), the fuel density is taken at the boiling point, and the fluid properties are evaluated at an average flame temperature used by [13] of $T_f = 1500$ K

$$\frac{L_f}{D} = C_f \left(\frac{\dot{m}_F c_p}{kD} \right), \quad C_f = 0.407 \frac{s}{Y_{ox,\infty}} \frac{T_{vap}}{T_f}, \quad (4)$$

where $Y_{ox,\infty}$ is the mass fraction of oxygen (taken here as air, 0.233), and T_{vap} is the vaporization or boiling point of the wax. Here, for tetracosane C_f is 2.68. Of course, for the current distributed nature of the candle fuel supply point, C_f is not definitive and might also depend on D/L .

From the conventional stagnant layer model for a one-dimensional diffusion flame sheet (e.g., [9,10]), the burning rate per unit area is expressed in terms of the B number:

$$\dot{m}''_F = \frac{h_c}{c_p} \ln(1 + B),$$

$$B \equiv \frac{Y_{ox,\infty} \Delta h_c / s - c_p (T_{vap} - T_\infty)}{h_{fg} + c_{liq} (T_{vap} - T_{melt})}. \quad (5)$$

The heat of gasification (the total denominator) here is composed of the heat of vaporization and the enthalpy increase of the liquid melt from the melt to the vaporization temperature. The B number is based on a flame sheet and soot, while it forms the basis of the visible flame, is not explicitly modeled.

In terms of Eq. (5) each fuel supply rate for the wick is given by

$$\dot{m}_{top} = \dot{m}''_{top} \frac{\pi}{4} D^2. \quad (6a)$$

and

$$\dot{m}_{cyl} = \dot{m}''_{cyl} \pi D L. \quad (6b)$$

The heat transfer coefficient for each orientation comes from the literature. Gebhart [14] gives the average heat transfer coefficient for a hot horizontal surface facing up, corresponding to the top of the candlewick:

$$Nu_{top} \equiv \frac{h_{c,top} D}{k} = 0.43 + 0.6 Ra^{1/4}. \quad (7)$$

The average result for the finite vertical cylinder comes from LeFevre and Ede [15]. For the candle, this applies for the vertical burn length, L_b .

$$Nu_{cyl} \equiv \frac{h_{c,cyl} L_b}{k} = \frac{L_b}{D} \left(0.52 + 0.547 \left(Ra \frac{D}{L_b} \right)^{1/4} \right). \quad (8)$$

The Rayleigh number is based on D and the properties are defined in terms of the film temperature computed accordingly to Gebhart [14] as the flame temperature (1400 °C) minus 0.38 times the difference between the flame temperature and the ambient temperature or 878 °C. For this study, that calculation for the data results in

$$Ra \equiv \frac{g \beta (T_f - T_\infty) D^3}{\alpha V} = 1.46 D^3 (\text{mm}). \quad (9)$$

It should be noted in Eqs. (8) and (9) that the Rayleigh number term is associated with boundary layer flow, and when it tends to zero pure dif-

fusion occurs. Combining Eqs. (4), (5), (6a), (6b), (7)–(9) gives a compact form for the flame length:

$$\frac{L_f}{D} = \pi C_f \ln(1 + B) (Nu_{top}/4 + Nu_{cyl}). \quad (10)$$

A prediction of the flame width at $x = L_b$ comes from the solution of the stagnant layer for cylindrical coordinates [10,12]:

$$\frac{W_f}{D} = \left(\frac{1 + B}{1 + Y_{ox,\infty}/s} \right)^{1/2}, \quad \lambda \equiv \left(\frac{c_p \dot{m}'_F}{2\pi k} \right)_{x=L_b}. \quad (11)$$

The burning rate per unit length, \dot{m}'_F , is the local value at the top of the wick and must be found accordingly from the local Nusselt number. This is given by LeFevre and Ede [15] as

$$Nu_{cyl,x} \equiv \frac{h_{c,cyl} x}{k} = \frac{x}{D} \left(0.52 + 0.41 \left(Ra \frac{D}{x} \right)^{1/4} \right). \quad (12)$$

and combining with Eq. (11) yields

$$\lambda = \frac{D}{2L_b} \ln(1 + B) Nu_{cyl,x=L_b}. \quad (13)$$

The values of C_f and λ are considered to be adjustable in these solutions in their application to the candle. In any case, the normalized flame height (L_f/D) and flame width (W_f/D) are to be functions of Ra and D/L , as well as B and s . Lacking complete data for paraffin (Table 1), its properties, (B and s), will be taken identical to n -tetracosane.

5. Results and discussion

Figure 7 shows the normalized flame length results for tetracosane data plotted against the computed values of Eq. (10) using the C_f as 2.68

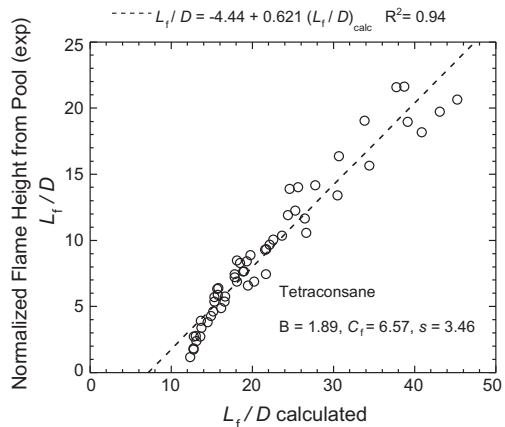


Fig. 7. Normalized flame length data and predictions from Eq. (10) for tetracosane.

from Eq. (4) and the property data of tetracosane. The Ra ranges from about 1 to 1000 for these data. A linear fit reveals that the theory overestimates the data by a factor of 0.62, and a “virtual origin L/D ” of 4.44 below the base of the wick is suggested. As expected, the Roper burner solution does not exactly apply to the distributive fuel supply of the candle. However adjusting the factor C_f by 0.62, and displacing the base of the wick is not so unreasonable for this approximate model. But navigating the solution through Eqs. (4), (5), (6a), (6b), (7)–(9) is still tedious.

For these data the Nu for the top and the cylinder both vary from about 1 to 5, and according to Eq. (10) the cylinder fuel supply should have a bigger effect on the flame height. Accordingly, the normalized flame height should increase with $Ra^{1/4}$ and $(L/D)^n$ with n ranging from about 3/4 to 1. As a consequence a simpler power law relationship was explored for the flame height with $Ra^{1/4}L/D$ as a correlating factor. These results are shown in Fig. 8 for both the tetracosane and the paraffin. The paraffin flames are shorter than the n -tetracosane, suggesting perhaps a smaller B number. From the data, these results are distinct for each wax. Both give power law correlations with good accuracy in terms of $Ra^{1/4}L/D - 2$. Indeed, these results indicate that the candle wick will have no flame for $Ra^{1/4}L/D < 2$, or $D(\text{mm}) < 0.88(D/L)^{4/3}$. The range of these data has D/L from about 0.1 to 2, and suggests wick diameters of about 0.9–2.2 mm, respectively, will not support a flame.

The solution for the width of the flame is more consistent for the candle flame, as the vertical boundary layer on a cylinder directly applies. Computed results are shown in Fig. 9 for tetracosane. The calculations were performed for the measured wick size for each data, and these results have been grouped into four classes of nearly con-

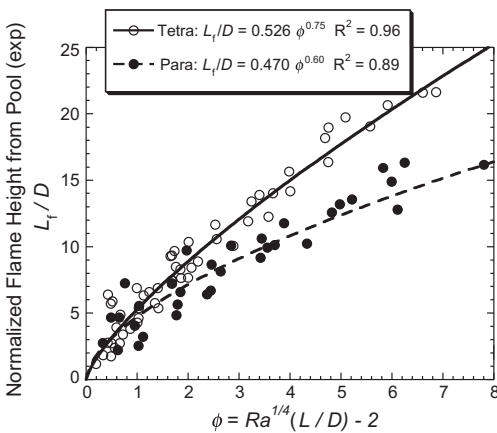


Fig. 8. Correlations for normalized flame height using Eq. (15).

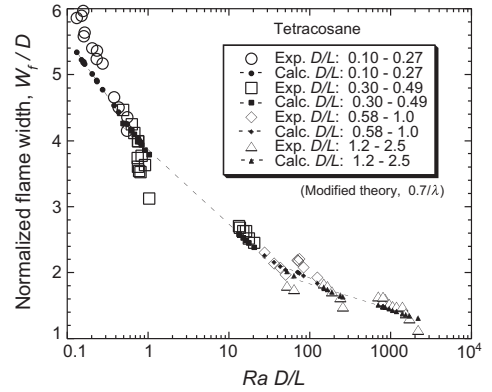


Fig. 9. Normalized flame width data and predictions for tetracosane by Eq. (14).

stant D/L ratios in Fig. 9. However, it was found that an adjustment was needed in the theory to produce more accurate results by introducing $0.7/\lambda$ for $1/\lambda$ in Eq. (11). The theory gives a solution in terms of RaD/L for each value D/L as a parameter, and dashed lines were traced through its constant D/L -classes to better identify their trends. Moreover, the experimental and theoretical results can be compared for each constant value of RaD/L and deviate by about 20%. Figure 10 shows the theory for tetracosane spanning the data values for constant D/L values of 0.1–2, and includes the paraffin data as well. The paraffin and tetracosane nearly follow the same trend, and suggest that the properties of tetracosane were satisfactory to predict the paraffin, as there is not a big difference in the wax properties. Numerical results from T’ien and coworkers [6,7] were also plotted for comparison in Fig. 10. They computed results for a wax of 80% pentacosane, and that

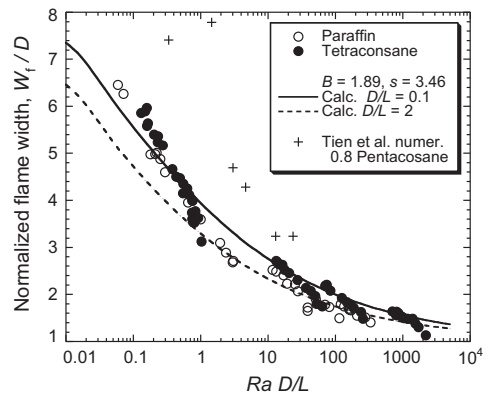


Fig. 10. Normalized flame width for tetracosane and paraffin with theory by Eq. (14) for D/L of 0.1 and 2; comparison to T’ien et al. predictions for 80% pentacosane [6,7].

should have similar properties to tetracosane. Their results follow the trend of these data but are higher. Perhaps the difference is due to wax types, or perhaps due to the complexities in modeling this problem from first principles. Here the approximate model has relied on accurate convective heat transfer correlations that have been supported by much data. Slight adjustments in the constants are common in heat transfer and might be attributed here to property variations more extreme for combustion problems.

6. Conclusions

Predictive results have been developed for the height and width of candle flames. The results apply to vertical, not bent, wicks. The wicks studied ranged in diameter from about 1 to 9 mm, and in height from about 2 to 10 mm, with aspect ratios of 0.1–2. A prediction, modified slightly, gives the width of the flame at the top of the wick as

$$W_f/D = 2.71^{0.70/\lambda} \quad (14)$$

with λ given in Eq. (13). The height of the flame, measured from the base of the wick, is given by

$$L_f/D = C(Ra^{1/4}(L/D) - 2)^n, \quad (15)$$

with C as 0.526 and 0.470, and n as 0.75 and 0.60 for tetracosane and paraffin, respectively. Also $Ra = 1.46 [D(\text{mm})]^3$ from Eq. (9).

References

- [1] M. Faraday, *The Chemical History of a Candle*, Dover Books, Mineola, NY, 2002.
- [2] F. Takahashi, in J. Jarosinski, B. Veyssiere (Eds.), *Combustion Phenomena*, CRC Press, Boca Raton, 2009, p. 170.
- [3] D.L. Dietrich, H.D. Ross, J.S. T'ien, P. Chang, Y. Shu, *Combust. Sci. Technol.* 156 (1) (2000) 1–24.
- [4] F.J. Kosdon, F.A. Williams, C. Buman, *Proc. Combust. Inst.* 12 (1968) 253–264.
- [5] N. Riley, *Proc. R. Soc. Lond. A* 442 (1993) 361–372.
- [6] A. Alsairafi, S.T. Lee, J.S. T'ien, *Combust. Sci. Technol.* 176 (12) (2004) 2165–2191.
- [7] M.P. Raju, J.S. T'ien, *Combust. Theory Model.* 12 (2) (2008) 367–388.
- [8] A. Hamins, M. Bundy, S. Dillon, *J. Fire Prot. Eng.* 15 (2005) 265–285.
- [9] D.B. Spalding, *Proc. Combust. Inst.* 4 (1953) 847–854.
- [10] P.J. Pagni, *Fire Safety J.* 3 (4) (1981) 273–285.
- [11] K.M. Allan, J.R. Kaminski, J.C. Bertrand, J. Head, P.B. Sunderland, *Combust. Sci. Technol.* 181 (2009) 800–811.
- [12] G.A. Tabaka, *Analysis and Measurement of Candle Flame Shapes*, M.S. Thesis, Department of FPE, University of Maryland, College Park, MD, 2008.
- [13] F.G. Roper, C. Smith, A.C. Cunningham, *Combust. Flame* 29 (1977) 227–234.
- [14] B. Gebhart, *Heat Transfer*, McGraw Hill, NY, 1971.
- [15] E.J. Le Fevre, A.J. Ede, in: *Proceedings of the 9th International Congress of Applied Mechanics*, vol. 4, 1957, pp. 175–183.